FOCUSING CHARGED PARTICLE BEAMS USING MULTIPOLE MAGNETS IN A BEAM TRANSPORT LINE

Y. Yuri, T. Yuyama, T. Ishizaka, I. Ishibori, and S. Okumura
Takasaki Advanced Radiation Research Institute, Japan Atomic Energy Agency,
1233 Watanuki-machi, Takasaki, Gunma, 370-1292, Japan.

Abstract

The transformation of the transverse intensity distribution due to the second-order sextupole and third-order octupole focusing force in a beam transport line is explored. As measures of the distribution transformation induced by the multipole magnet, the displacement of the beam centroid and the change in the rms beam size have been derived analytically using the first-order and second-order moments of the intensity distribution function. It is numerically and experimentally verified how the transverse distribution of the beam is transformed by the multipole magnets. As an application of the distribution transformation by nonlinear focusing, an ion beam with an almost uniform transverse intensity distribution is formed from a Gaussian-like beam using multipole magnets for large-area uniform irradiation at the cyclotron facility in Japan Atomic Energy Agency (JAEA).

INTRODUCTION

The transverse phase-space distribution of a charged-particle beam is deformed once some nonlinear force of a multipole magnet is applied to the beam. Consequently, the spatial distribution of the beam is also changed from the original one. The nonlinear focusing force produced by multipole magnets can be employed to form a beam with a uniform transverse intensity distribution in the beam transport line [1-5]. Uniform ion beams have been actually formed by the third-order forces from octupole magnets for various applications [6-9].

In this paper, the transformation of the transverse intensity distribution is explored when the beam is focused by a sextupole or octupole magnet in a beam transport line. Analytical expressions on the centroid displacement and envelope of the beam are derived as a function of the multipole strength from the first-order and second-order moments [10]. Single-particle tracking simulations were performed to see how the beam distribution is transformed by the multipole force and to verify the theoretical consideration. Furthermore, an experiment with proton beams was also carried out to form a uniform distribution using multipole magnets at the JAEA azimuthally-varying-field (AVF) cyclotron facility.

THEORETICAL ANALYSIS OF NONLINEAR FOCUSING

Assume that a charged particle travels along a linear beam transport line composed of quadrupole and multipole magnets. We here consider only one transverse direction of motion in order to eliminate the complexity of the analysis, although two transverse degrees of particle motion are inevitably coupled through the multipole magnet. Actually, it is possible to suppress the betatron coupling by properly adjusting the beam optics as explained later (See Fig. 1). According to Ref. [5], the on-target real-space distribution ρ_t of the beam focused by a multipole magnet can be determined analytically. It is given, using the initial distribution ρ_0 at the multipole magnet (number of poles: $2n$, integrated strength: K_{2n}) as follows:

$$\rho_t = \rho_0 \left/ \left[\sqrt{\frac{\beta_t}{\beta_0}} \cos\phi - \sqrt{\beta_0\beta_t} \sin\phi \frac{K_{2n}}{(n-2)!} x_0^{n-2} \right] \right. , \quad (1)$$

where β_0 and β_t are, respectively, the beta functions at the multipole magnet and at the target, ϕ is the betatron phase advance from the multipole magnet to the target, and x_0 is the particle's coordinate at the multipole magnet.

We here consider the centroid displacement and the root-mean-square (rms) radius of the on-target beam. Such characteristics of the distribution can be described using the first-order and second-order moments:

$$\langle x_t \rangle = \int x_t \rho_t dx_t, \quad \left\langle \left(x_t - \langle x_t \rangle \right)^2 \right\rangle = \int \left(x_t - \langle x_t \rangle \right)^2 \rho_t dx_t, \quad (2)$$

where x_t is the particle's coordinate at the target. These moments can be analytically integrated, incorporating Eq. (1) and assuming the initial Gaussian distribution, $\rho_0 = 1 \left/ \sqrt{2\pi\varepsilon\beta_0} \right. \mathrm{Exp}\left[-x_0^2 / (2\varepsilon\beta_0) \right]$, with the rms emittance ε of the beam. We thus have the beam centroid displacement X on the target, which corresponds to the first-order moment, and the rms beam radius σ, which is the square root of the second-order moment. For the sextupole-focusing ($n=3$) case [10],

$$X \equiv \langle x_t \rangle = -\frac{1}{2}\varepsilon\beta_0\sqrt{\beta_0\beta_t} K_6 \sin\phi, \quad (3)$$

$$\sigma \equiv \sqrt{\left\langle (x_t - X)^2 \right\rangle} = \sqrt{\varepsilon\beta_t} \sqrt{1 + \frac{1}{2}\varepsilon\beta_0^3 K_6^2 \tan^2\phi} \, |\cos\phi|. \quad (4)$$

As can be seen from Eqs. (3) and (4), the centroid displacement X is proportional to the sextupole force, and the rms size σ is always increased by sextupole focusing. For the octupole-focusing ($n=4$) case,

$$X = 0, \quad (5)$$

$$\sigma = \sqrt{\varepsilon\beta_t} \sqrt{1 - \varepsilon\beta_0^2 K_8 \tan\phi + \frac{5}{12}\left(\varepsilon\beta_0^2 K_8 \tan\phi\right)^2} \, |\cos\phi|. \quad (6)$$

The beam size can be reduced by an octupole magnet with a proper field polarity.

Note that, similarly, the beam centroid displacement and rms beam size on the target can be analytically obtained when the beam is focused by other higher-order multipole magnet.
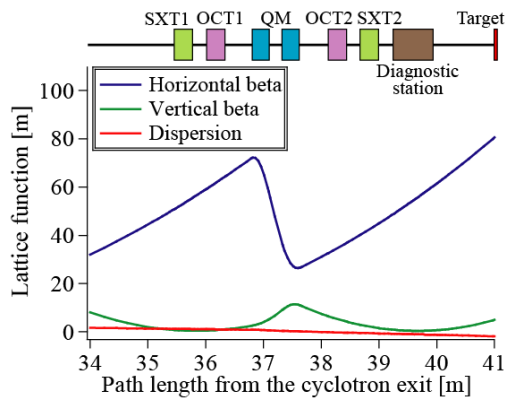
Figure 1: Schematic layout of magnets and the lattice functions around the end of the beam line at the JAEA AVF cyclotron. QM, SXT1 (SXT2), and OCT1 (OCT2) denote the quadrupole, sextupole, and octupole magnets, respectively. The axial length of the multipole magnets is 0.30 m. The beam-optical parameters have been adjusted so that the horizontal beta function is much larger than the vertical one at the multipole magnet locations for the reduction of the betatron coupling.

NUMERICAL SIMULATION

Single-particle tracking simulations were performed to confirm the analytical result in the previous section. We considered an actual lattice layout of the beam transport system equipped with sextupole and octupole magnets at the JAEA AVF cyclotron [11], as shown in Fig. 1. Only the horizontal degree of freedom of the beam motion was considered in the present simulation so that numerical results can be compared with the analytical results. As an initial condition of the beam, a beam whose distribution is Gaussian and horizontal rms emittance is 10π mm mrad was assumed.

Sextupole Focusing

When no sextupole force is applied to the beam, the on-target distribution is elliptical in the phase space and Gaussian in the real space. Once the sextupole magnet is turned on, the elliptical phase-space profile is bent into a *hook-like* shape by the sextupole force, as shown in Fig. 2. Seen in the real-space profile, particles are nonlinearly deflected toward one side. As a result, the on-target spatial distribution has a long tail on the side and a steep peak on the other side. The tilt of the sloped distribution is reversed when the polarity of the applied sextupole force is reversed. We have confirmed that the displacement of the beam centroid position and the rms beam size, obtained from the on-target particle distribution, agree fairly well with the theoretical predictions in Eqs. (3) and (4), respectively.

It is worthy to mention the transformation of the distribution when the beam is focused by sextupole magnets twice along the beam line. When the two sextupole magnets are turned on with proper strengths and polarities, both side tails of the Gaussian distribution can be folded into the inside, and a uniform distribution
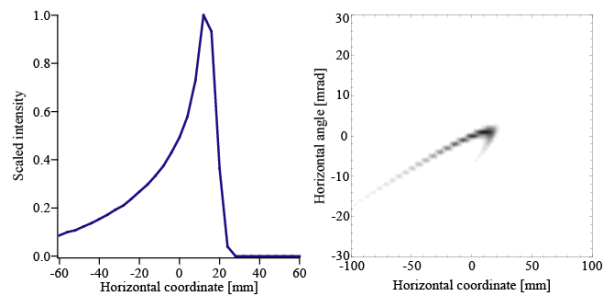
Figure 2: On-target real-space and phase-space distributions of the beam focused by a sextupole magnet, SXT1. The gradient of the sextupole magnet is set at 19 m^{-3}. The number of particles used in the simulation is 10^6.
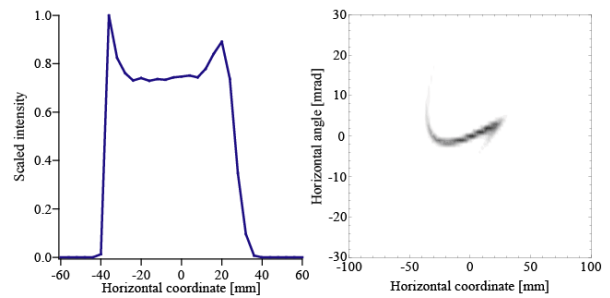
Figure 3: On-target real-space and phase-space distributions of the beam. The simulation parameters are the same as those in Fig. 2 except that another sextupole magnet SXT2 has been additionally turned on at the gradients of -52 m^{-3}.
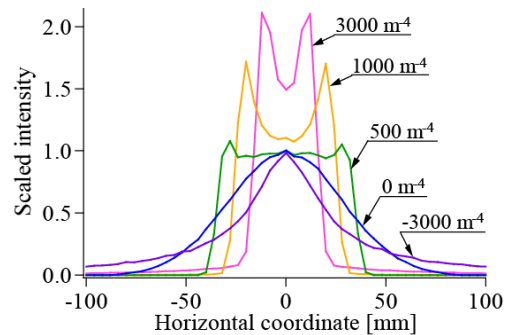
Figure 4: On-target real-space distributions of the beam focused by an octupole magnet, OCT1 with several different strengths.

can be formed, as shown in Fig. 3 [5]. This demonstrates that the combined use of two sextupole magnets has a tail-folding effect similar to octupole magnets.

Octupole Focusing

Figure 4 shows the on-target spatial distributions of the beams focused with several different octupole strengths. With a proper polarity of the magnet, the tail of the Gaussian beam is folded, and thus the resultant distribution has a steep edge. An almost uniform distribution can be formed at a specific octupole strength. The phase-space profile of the octupole-focused beam is deformed into an "S" shape [5]. The dependence of the rms beam size on the octupole strength agreed with the theoretical prediction Eq. (6).
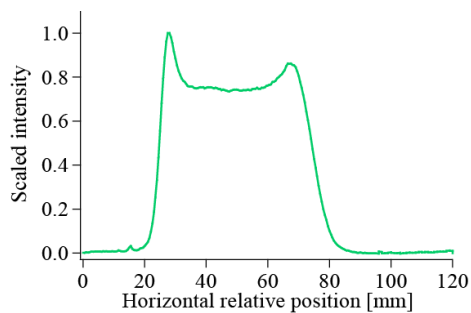
Figure 5: Horizontal relative intensity distributions of the proton beam measured using a radiochromic dosimetry film on the target [12]. The beam was focused by two sextupole magnets SXT1 and SXT2 with the field gradients of 41 m^{-3} and -54 m^{-3}, respectively.

Figure 6: Spatial intensity distributions of the proton beam measured using a radiochromic film on the target. The beam was focused by two octupole magnets OCT1 and OCT2. The rms uniformity of the central 9-cm-square region is 5%.

EXPERIMENT

The transformation of the distribution was also experimentally investigated using 10-MeV proton beams from the JAEA AVF cyclotron for future applications such as uniform-beam irradiation. In order to suppress the betatron coupling induced by multipole magnets as low as possible, we have chosen the beam-optical parameters as follows: The horizontal beta function is set much larger than the vertical one at the multipole magnets as shown in Fig. 1. It has been confirmed that no significant coupling effect can be seen in the vertical direction.

The problem here is that the intensity distribution of the beam extracted from the cyclotron is often asymmetric and complicated. In order to clarify the distribution transformation by the multipole magnet, the initial beam distribution was smoothed into a Gaussian-like distribution by a thin Al foil through multiple Coulomb scattering in the first straight section of the beam line after the cyclotron exit [9].

Sextupole Focusing

The deformation of the transverse distribution, similar to Fig. 2, was observed by exciting either SXT1 or SXT2. Furthermore, we demonstrated, as shown in Fig. 5, that the transverse distribution could be transformed into a uniform one by choosing the strengths and polarities of the two sextupole magnets properly. The rms uniformity of the beam is 3% in the central flattop region of the measured distribution. The use of sextupole magnets for uniform-beam formation is unique in that it is less susceptible to the beam misalignment, as compared to the octupole-focusing case [10].

Octupole Focusing

We here adopted a lattice parameter different from Fig. 1 for the formation of a large-area two-dimensionally uniform beam, which is our main purpose of the present study. In the present case, the first (second) octupole magnet OCT1 (OCT2) folds the horizontal (vertical) tail of the Gaussian-like beam, and, thereby, a large-area uniform beam can be formed on the target, as shown in Fig. 6.
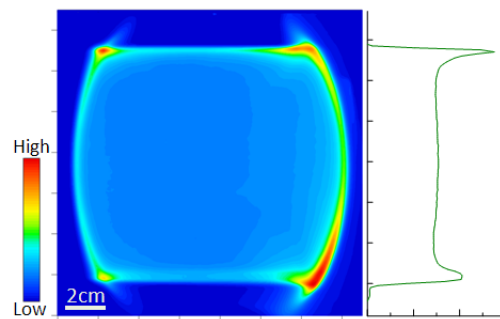
SUMMARY

We explored the effects of sextupole and octupole focusing on the transverse beam intensity distribution in the beam transport system through theoretical analysis, numerical simulations and experiments. The changes in the centroid position and rms size of the beam were analytically shown. The validity of the theoretical consideration was tested through single-particle tracking simulations. In the experimental study at the JAEA AVF cyclotron, one-dimensional and two-dimensional uniform beams were formed using two sextupole and octupole magnets respectively. Such an ion beam with a specific transverse distribution tailored by the nonlinear focusing force has been employed for various particle-beam applications in materials science [9].

REFERENCES

[1] P. F. Meads, Jr., IEEE Trans. Nucl. Sci. **30** (1983) 2838.

[2] B. Sherril et al., Nucl. Instrum. Methods Phys. Res. Sect. B **40/41** (1989) 1004.

[3] Y. K. Batygin, Nucl. Instrum. Methods Phys. Res. Sect. B **79** (1993) 770.

[4] F. Meot and T. Aniel, Nucl. Instrum. Methods Phys. Res., Sect. A **379** (1996) 196.

[5] Y. Yuri et al., Phys. Rev. ST Accel. Beams **10** (2007) 104001.

[6] S. Richter et al., Proc. 8th European Particle Accelerator Conference, Paris, France, 2002, p. 1181.

[7] N. Tsoupas et al., Phys. Rev. ST Accel. Beams **10** (2007) 024701.

[8] A. Bogdanov et al., Proc. 2007 Particle Accelerator Conf., Albuquerque, USA, 2007, p. 1748.

[9] Y. Yuri et al., Nucl. Instrum. Methods Phys. Res. Sect. A **642** (2011) 10.

[10] Y. Yuri et al., J. Phys. Soc. Jpn. **81** (2012) 064501.

[11] K. Arakawa et al., Proc. 13th Int. Conf. on Cyclotrons and their Applications, Vancouver, Canada, 1992, p. 119.

[12] T. Agematsu et al., Radioisotopes **57** (2008) 87 [in Japanese].